

Real-time Machine Learning-Based CLBF-MPC of Nonlinear Systems ^{*}

Zhe Wu ^{*} David Rincon ^{*} Panagiotis D. Christofides ^{**}

^{*} *Department of Chemical and Biomolecular Engineering, University of California, Los Angeles, CA, 90095-1592, USA (email: wuzhe@g.ucla.edu)*

^{**} *Department of Chemical and Biomolecular Engineering and Department of Electrical and Computer Engineering, University of California, Los Angeles, CA 90095-1592, USA (e-mail: pdc@seas.ucla.edu)*

Abstract: In this work, a real-time Control Lyapunov-Barrier Function-based model predictive control (CLBF-MPC) system using recurrent neural network (RNN) models is developed for a general class of nonlinear systems to ensure closed-loop stability and operational safety accounting for time-varying disturbances. An RNN model is first constructed for the nominal system (i.e., without disturbances) and utilized in the design of CLBF-MPC to provide state prediction. Subsequently, to improve the closed-loop performance in terms of operational safety and stability in the presence of disturbances, online learning of RNN models is incorporated within the real-time implementation of CLBF-MPC to update the RNN models using the most recent process measurement data. The proposed adaptive machine-learning-based CLBF-MPC method is evaluated using a nonlinear chemical process example.

Keywords: Machine learning; Model predictive control; Control Lyapunov-Barrier Functions; Nonlinear systems; Chemical processes

1. INTRODUCTION

Recurrent neural networks (RNN), a class of artificial neural networks where feedback loops are employed to introduce past information into the network, has demonstrated its capability in approximating complex, nonlinear dynamic systems in the discipline of data-driven modeling, (e.g., You and Nikolaou [1993], Kosmatopoulos et al. [1995], Trischler and D'Eleuterio [2016]). As RNN can provide an accurate process model for model-based optimization of chemical processes, e.g., model predictive control (MPC) when a first-principles model is unavailable, RNN modeling methods have been recently incorporated in the design of MPC to operate a nonlinear process at the steady-state while optimizing process dynamic performance. For example, it is demonstrated in Wu et al. [2019c] that desired closed-loop performance in terms of guaranteed stability, optimal response, and smooth control actions can be achieved under the MPC using an ensemble of RNN models that well capture process nonlinear dynamics. In addition to process stability, another issue that is important in chemical process operation and has attracted a lot of attention in the engineering community is process operational safety. To ensure that a process is being operated in safe operating conditions for all times, safety protection systems including process control systems, alarms systems and emergency shut down systems have been developed and widely-used in industry. Specifically, advanced process control systems at the lowest

level of safety protection system need to be designed to account for safety considerations such as operating the system safely and avoiding triggering alarms systems too frequently.

To incorporate process safety constraints into MPC design, Control Lyapunov-Barrier functions (CLBF) (Romdlony and Jayawardhana [2016]) that are designed based on Control Lyapunov functions and Control barrier functions (Ames et al. [2016], Jankovic [2017]) have been developed and utilized in MPC to stabilize the closed-loop state at its steady-state while avoiding unsafe operating regions in state-space. It has been demonstrated in Wu et al. [2019a] that under CLBF-MPC, recursive feasibility of the optimization problem of CLBF-MPC, closed-loop stability and process operational safety can be guaranteed simultaneously for nonlinear processes.

Despite the successful applications of RNNs in model-based controllers, there is an increasing need to address online learning of machine learning models as all real-world processes are changing over time due to external disturbances and internal variations (e.g., catalyst deactivation). To that end, adaptive machine-learning-based MPC has been developed in Wu et al. [2019b] to update RNN models using real-time process data for nonlinear processes subject to time-varying disturbances. Motivated by the above, in this work, we develop a real-time adaptive CLBF-based MPC that updates RNN models following the error-triggered mechanism that has been proposed in Wu et al. [2019b]. Specifically, an RNN-based CLBF-MPC is first developed to derive closed-loop stability and safety for

^{*} Financial support from the National Science Foundation and the Department of Energy is gratefully acknowledged.

the nominal system. Based on that, online learning of RNN models is incorporated in the real-time implementation of CLBF-MPC to safely operate the system and drive the state to its steady-state in the presence of disturbances.

2. PRELIMINARIES

2.1 Notation

The notation $|\cdot|$ is used to denote the Euclidean norm of a vector. x^T denotes the transpose of x . The notation $L_f V(x)$ denotes the standard Lie derivative $L_f V(x) := \frac{\partial V(x)}{\partial x} f(x)$. Set subtraction is denoted by " \setminus ", i.e., $A \setminus B := \{x \in \mathbf{R}^n \mid x \in A, x \notin B\}$. \emptyset signifies the empty set. The function $f(\cdot)$ is of class \mathcal{C}^1 if it is continuously differentiable in its domain. A continuous function $\alpha : [0, a] \rightarrow [0, \infty)$ is said to belong to class \mathcal{K} if it is strictly increasing and is zero only when evaluated at zero.

2.2 Class of Systems

The class of continuous-time nonlinear systems considered is described by the first-order nonlinear ordinary differential equations as follows:

$$\dot{x} = f(x) + g(x)u + h(x)w, \quad x(t_0) = x_0 \quad (1)$$

where $x \in \mathbf{R}^n$ is the state vector, $u \in \mathbf{R}^m$ is the manipulated input vector, and $w \in W$ is the disturbance vector bounded by $W := \{w \in \mathbf{R}^q \mid |w| \leq w_m, w_m \geq 0\}$. The control action constraint is defined by $u \in U := \{u_i^{\min} \leq u_i \leq u_i^{\max}, i = 1, \dots, m\} \subset \mathbf{R}^m$. $f(\cdot)$, $g(\cdot)$, $h(\cdot)$ are sufficiently smooth vector and matrix functions of dimensions $n \times 1$, $n \times m$, and $n \times q$, respectively. Throughout the manuscript, the initial time t_0 is taken to be zero ($t_0 = 0$), and it is assumed that $f(0) = 0$, and thus, the origin is a steady-state of the nominal system of Eq. 1 with $w(t) \equiv 0$, (i.e., $(x_s^*, u_s^*) = (0, 0)$).

2.3 Stabilizability Assumptions and Safety Considerations

A positive definite Control Lyapunov function (CLF) V that satisfies the small control property (i.e., for every $\varepsilon > 0$, $\exists \delta > 0$, s.t. $\forall x \in \mathcal{B}_\delta(0)$, there exists u that satisfies $|u| < \varepsilon$ and $L_f V(x) + L_g V(x)u < 0$, Sontag [1989]) and the following condition is assumed to exist for the nominal system of Eq. 1 with $w(t) \equiv 0$:

$$L_f V(x) < 0, \forall x \in \{z \in \mathbf{R}^n \setminus \{0\} \mid L_g V(z) = 0\} \quad (2)$$

The above CLF assumption implies that there exists a stabilizing feedback control law $\Phi(x) \in U$ for the nominal system of Eq. 1 (i.e., $w(t) \equiv 0$) that renders the origin of the closed-loop system asymptotically stable for all x in a neighborhood of the origin.

Additionally, we assume that there exists a set $\mathcal{D} \subset \mathbf{R}^n$ in state-space within which it is unsafe for the system to be operated, and a safe stability region \mathcal{U} such that $\mathcal{U} \cap \mathcal{D} = \emptyset$ and $\{0\} \subset \mathcal{U}$, within which closed-loop stability and process operational safety are achieved simultaneously in the following sense:

Definition 1. (Wu and Christofides [2020]) Consider the system of Eq. 1 and input constraints $u \in U$. If there exists a control law $u = \Phi(x) \in U$ such that for any initial state $x(t_0) = x_0 \in \mathcal{U}$, $x(t)$ remains inside \mathcal{U} , $\forall t \geq 0$, and the origin of the closed-loop system of Eq. 1 can be rendered asymptotically stable, we say that the control law $\Phi(x)$

maintains the process state within a safe stability region \mathcal{U} at all times.

2.4 Recurrent Neural Network

The following recurrent neural network (RNN) model is developed to approximate the nonlinear dynamics of the system of Eq. 1:

$$\dot{\hat{x}} = F_{nn}(\hat{x}, u) := A\hat{x} + \Theta^T y \quad (3)$$

where $\hat{x} \in \mathbf{R}^n$ is the RNN state vector and $u \in \mathbf{R}^m$ is the manipulated input vector. $y = [y_1, \dots, y_n, y_{n+1}, \dots, y_{m+n}] = [\sigma(\hat{x}_1), \dots, \sigma(\hat{x}_n), u_1, \dots, u_m] \in \mathbf{R}^{n+m}$ is a vector of both the network state \hat{x} and the input u , where $\sigma(\cdot)$ is the nonlinear activation function (e.g., a sigmoid function $\sigma(x) = 1/(1 + e^{-x})$). A is a diagonal coefficient matrix, i.e., $A = \text{diag}\{-a_1, \dots, -a_n\} \in \mathbf{R}^{n \times n}$ with $a_i > 0$, $i = 1, \dots, n$, and $\Theta = [\theta_1, \dots, \theta_n] \in \mathbf{R}^{(m+n) \times n}$ with $\theta_i = b_i[w_{i1}, \dots, w_{i(m+n)}]$, $i = 1, \dots, n$. w_{ij} is the weight connecting the j th input to the i th neuron where $i = 1, \dots, n$ and $j = 1, \dots, (m+n)$. It is noted that the RNN model of Eq. 3 is an input-affine system, and therefore, it can be written in the form that is similar to Eq. 1:

$$\dot{\hat{x}} = \hat{f}(\hat{x}) + \hat{g}(\hat{x})u \quad (4)$$

where $\hat{f}(\cdot)$ and $\hat{g}(\cdot)$ can be derived from the coefficient matrices A and Θ in Eq. 3 and are assumed to be sufficiently smooth. The development of an RNN model follows the two steps (data collection and training process) as discussed in Wu et al. [2019c]. Additionally, to ensure that the RNN model of Eq. 3 has the same steady-state as the nonlinear system of Eq. 1, during the training process, the modeling error ν is required to be bounded by $|\nu| = |F(x, u, 0) - F_{nn}(x, u)| \leq \gamma|x| \leq \nu_m$, $\gamma > 0$, where $\nu_m > 0$ is the upper bound within the operating region. Similarly, we assume that there exists a Control Lyapunov function V and a stabilizing controller $u = \Phi_{nn}(x) \in U$ that renders the origin of the RNN system of Eq. 3 asymptotically stable.

2.5 Stabilization and Safety via Control Lyapunov-Barrier Function

Control Lyapunov-Barrier Function (CLBF) has been utilized in Romdlony and Jayawardhana [2016], Wu et al. [2019a] to design a stabilizing controller that drives the state of the nonlinear system of Eq. 1 to the origin while avoiding the unsafe region in state-space. Specifically, the definition of constrained CLBFs $W_c(x)$ that are designed for the RNN system of Eq. 3 subject to input constraints is as follows:

$$W_c(x) > \rho, \quad \forall x \in \mathcal{D} \subset \phi_{uc} \quad (5a)$$

$$L_{\hat{f}} W_c(x) < 0,$$

$$\forall x \in \{z \in \phi_{uc} \setminus (\mathcal{D} \cup \{0\} \cup \mathcal{X}_e) \mid L_{\hat{g}} W_c(z) = 0\} \quad (5b)$$

$$\mathcal{U}_\rho := \{x \in \phi_{uc} \mid W_c(x) \leq \rho\} \neq \emptyset \quad (5c)$$

where $\rho \in \mathbf{R}$, and $\mathcal{X}_e := \{x \in \phi_{uc} \setminus (\mathcal{D} \cup \{0\}) \mid \partial W_c(x)/\partial x = 0\}$ is a set of states for the RNN model of Eq. 4 where $L_{\hat{f}} W_c(x) = 0$ (for $x \neq 0$) due to $\partial W_c(x)/\partial x = 0$. \hat{f} and \hat{g} are from the RNN model in the form of Eq. 4. The construction method of the constrained CLBF of Eq. 5 can be found in Romdlony and Jayawardhana [2016] and Wu et al. [2019a], in which a control Lyapunov function and

a control barrier function are designed separately and combined together through weighted average.

A feedback control law $u = \Phi_{nn}(x) \in U$ that renders the origin exponentially stable within an open neighborhood ϕ_{uc} that includes the origin in its interior is assumed to exist for the RNN system of Eq. 3 (also in the form of Eq. 4) in the sense that there exists a C^1 constrained Control Lyapunov-Barrier function $W_c(x)$ that has a minimum at the origin and satisfies the following inequalities $\forall x \in \phi_{uc}$:

$$\hat{c}_1|x|^2 \leq W_c(x) - \rho_0 \leq \hat{c}_2|x|^2, \quad (6a)$$

$$\frac{\partial W_c(x)}{\partial x} F_{nn}(x, \Phi_{nn}(x)) \leq -\hat{c}_3|x|^2, \forall x \in \phi_{uc} \setminus \mathcal{B}_\delta(x_e) \quad (6b)$$

$$\left| \frac{\partial W_c(x)}{\partial x} \right| \leq \hat{c}_4|x| \quad (6c)$$

where $\hat{c}_j(\cdot)$, $j = 1, 2, 3, 4$ are positive real numbers, $W_c(0) = \rho_0$ is the global minimum value of $W_c(x)$ in D , and $\mathcal{B}_\delta(x_e)$ is a small neighborhood around $x_e \in \mathcal{X}_e$. $F_{nn}(x, u)$ is the RNN system of Eq. 3. The universal Sontag controller Lin and Sontag [1991] with $W_c(x)$ replacing the Lyapunov function $V(x)$ can be used as a stabilizing control law $\Phi_{nn}(x)$ that satisfies the conditions in Eq. 6. Additionally, by continuity and the smoothness assumed for f, g and h in the nonlinear system of Eq. 1, there exist positive constants M, L_x, L_w, L'_x, L'_w such that the following inequalities hold for all $x, x' \in \mathcal{U}_\rho, u \in U$, and $w \in W$:

$$|F(x, u, w)| \leq M \quad (7a)$$

$$|F(x, u, w) - F(x', u, 0)| \leq L_x|x - x'| + L_w|w| \quad (7b)$$

$$\left| \frac{\partial W_c(x)}{\partial x} F(x, u, w) - \frac{\partial W_c(x')}{\partial x} F(x', u, 0) \right| \leq L'_x|x - x'| + |L'_w|w_m| \quad (7c)$$

The following theorem is established to demonstrate that in the presence of an unsafe region \mathcal{D} , closed-loop stability and operational safety are achieved simultaneously for the RNN system of Eq. 3 under the CLBF-based controller.

Theorem 1. Consider that a constrained CLBF $W_c(x): \mathbf{R}^n \rightarrow \mathbf{R}$ that has a minimum at the origin and meets the conditions of Eq. 5, exists for the RNN system of Eq. 3. The controller $u = \Phi_{nn}(x) \in U$ that satisfies Eq. 6 guarantees that the closed-loop state stays in \mathcal{U}_ρ and avoids the unsafe region \mathcal{D} for all times for any $x_0 \in \mathcal{U}_\rho$. Additionally, in the presence of an unbounded unsafe region, the origin can be rendered exponentially stable under $u = \Phi_{nn}(x) \in U$, for all $x_0 \in \mathcal{U}_\rho$, while discontinuous control actions $u = \bar{u}(x) \in U$ are required at stationary points x_e ($x_e \neq 0$) for a bounded unsafe region in state-space within \mathcal{U}_ρ .

Proof: It is noted in Wu et al. [2019a] that the unsafe regions \mathcal{D} can be categorized as bounded unsafe regions (e.g., a set of unsafe operating conditions in a chemical reactor) and unbounded unsafe regions (e.g., obstacle avoidance in motion planning). Specifically, it is pointed out in Wu et al. [2019a] that in the case of an unbounded unsafe region, the origin (i.e., the steady-state of the nonlinear system of Eq. 1) is the unique stationary point in state-space, and therefore, closed-loop stability and process operational safety can be readily derived under the controller $u = \Phi_{nn}(x) \in U$. However, in the presence

of a bounded unsafe region, there exist stationary points (other than the origin) in state-space (i.e., \mathcal{X}_e in Eq. 5b), and therefore, the stationary points need to be designed to be saddle points and discontinuous control actions will be applied at saddle points to drive the state away from them in the direction of decreasing $W_c(x)$ to ensure closed-loop stability and safety. The detailed proofs for both bounded and unbounded unsafe regions can be found in Wu and Christofides [2020], and are omitted here.

3. REAL-TIME CLBF-BASED MPC USING RNNs

In this section, we present the formulation of CLBF-MPC using an RNN model and demonstrate that closed-loop stability and safety can be achieved simultaneously under CLBF-MPC for the nominal system of Eq. 1 (i.e., $w(t) \equiv 0$). Subsequently, in the presence of time-varying disturbances $w(t)$, online learning of RNN models is employed within CLBF-MPC via an error-triggered mechanism to improve RNN prediction accuracy using the most recent process data.

3.1 Formulation of CLBF-MPC

The CLBF-MPC using an RNN model is represented by the following optimization problem Wu et al. [2019a]:

$$\mathcal{J} = \min_{u \in S(\Delta)} \int_{t_k}^{t_{k+N}} L(\tilde{x}(t), u(t)) dt \quad (8a)$$

$$\text{s.t. } \dot{\tilde{x}}(t) = F_{nn}(\tilde{x}(t), u(t)) \quad (8b)$$

$$\tilde{x}(t_k) = x(t_k) \quad (8c)$$

$$u(t) \in U, \forall t \in [t_k, t_{k+N}) \quad (8d)$$

$$\begin{aligned} \dot{W}_c(x(t_k), u(t_k)) &\leq \dot{W}_c(x(t_k), \Phi_{nn}(t_k)) \\ &\text{if } W_c(x(t_k)) > \rho_{nn} \text{ and } x(t_k) \notin \mathcal{B}_\delta(x_e) \end{aligned} \quad (8e)$$

$$\begin{aligned} W_c(\tilde{x}(t)) &\leq \rho_{nn}, \forall t \in [t_k, t_{k+N}), \\ &\text{if } W_c(x(t_k)) \leq \rho_{nn} \end{aligned} \quad (8f)$$

$$\begin{aligned} W_c(\tilde{x}(t)) &< W_c(x(t_k)) - f_e(t - t_k), \forall t \in (t_k, t_{k+N}), \\ &\text{if } x(t_k) \in \mathcal{B}_\delta(x_e) \end{aligned} \quad (8g)$$

where $\tilde{x}(t)$, $S(\Delta)$ and N are the predicted state trajectory, the set of piecewise constant functions with period Δ , and the number of sampling periods in the prediction horizon, respectively. The cost function $L(\tilde{x}(t), u(t))$ is generally in a quadratic form that has the minimum value at the equilibrium of the system of Eq. 1 (e.g., $|\tilde{x}(t)|_{Q_L}^2 + |u(t)|_{R_L}^2$, where Q_L and R_L are positive definite matrices). The RNN model of Eq. 3 is utilized to predict states $\tilde{x}(t)$ over $t \in [t_k, t_{k+N})$. The objective function of Eq. 8a is the time integral of $L(\tilde{x}(t), u(t))$ over the prediction horizon. The input constraints of Eq. 8d are applied over the entire prediction horizon. The state measurement of Eq. 8c at $t = t_k$ is taken as the initial condition for the RNN models of Eq. 8b. The constraint of Eq. 8e forces $W_c(\tilde{x})$ along the predicted state trajectories to decrease at least at the rate under the CLBF-based controller $u = \Phi_{nn}(x) \in U$ when $W_c(x(t_k)) > \rho_{nn}$ and $x(t_k) \notin \mathcal{B}_\delta(x_e)$. If $W_c(x(t_k)) \leq \rho_{nn}$, the constraint of Eq. 8f is activated to maintain the predicted state of the RNN system within $\mathcal{U}_{\rho_{nn}}$ such that the closed-loop state of the nonlinear system of Eq. 1 is bounded $\mathcal{U}_{\rho_{min}}$. Additionally, if $x(t_k) \in \mathcal{B}_\delta(x_e)$, the constraint of Eq. 8g decreases $W_c(x)$ over the prediction horizon such that the state can escape from saddle points

x_e within finite sampling steps, where $f_e(t)$ is a function that represents the difference between predicted value of $W_c(\hat{x})$ and actual value of $W_c(x)$ due to a nonzero modeling error. The state measurements of the closed-loop system of Eq. 1 are assumed to be available at each sampling time. The CLBF-MPC optimization problem of Eq. 8 calculates an optimal input sequence but only sends the first control action to the control actuators to be applied over the next sampling period.

The theorem below demonstrates that under the CLBF-MPC of Eq. 8, closed-loop stability and process operational safety are achieved simultaneously for the nominal system of Eq. 1 (i.e., $w(t) \equiv 0$) in the sense that the closed-loop state is bounded in the safe operating region \mathcal{U}_ρ for all times, and is ultimately bounded in a small neighborhood $\mathcal{U}_{\rho_{min}}$ around the origin.

Theorem 2. Consider the nominal system of Eq. 1 (i.e., $w(t) \equiv 0$) with a constrained CLBF W_c that satisfies Eq. 5 and has a minimum at the origin. Given any initial state $x_0 \in \mathcal{U}_\rho$, it is guaranteed that the CLBF-MPC optimization problem of Eq. 8 can be solved with recursive feasibility for all times. Additionally, under the sample-and-hold implementation of CLBF-MPC based on an RNN model that satisfies $|\nu| = |F(x, u, 0) - F_{nn}(x, u)| \leq \gamma|x| \leq \nu_m$, it is guaranteed that for any $x_0 \in \mathcal{U}_\rho$, the state is bounded in \mathcal{U}_ρ , $\forall t \geq 0$, and ultimately converges to $\mathcal{U}_{\rho_{min}}$ as $t \rightarrow \infty$.

Proof: The proof can be found in Wu and Christofides [2020], and is omitted here.

3.2 Error-triggered On-line Learning of RNNs

Now we consider the nonlinear system of Eq. 1 subject to bounded time-varying disturbances (i.e., $|w(t)| \leq w_m$) that cannot be fully eliminated by the sample-and-hold implementation of CLBF-MPC using the RNN models that are developed for the nominal system of Eq. 1 (i.e., $w(t) \equiv 0$). In this case, the closed-loop system of Eq. 1 may be rendered unstable under the CLBF-MPC using the initial RNN model for all times. To account for the impact of disturbances in the prediction of the CLBF-MPC of Eq. 8, the RNN model of Eq. 8b needs to be updated via on-line learning using the most recent data to capture the nonlinear dynamics of the system of Eq. 1 subject to the time-varying disturbances $w(t)$. Specifically, based on the error-triggering mechanism in Wu et al. [2019b], the following moving horizon error metric $E_{rnn}(t_k)$ is developed to indicate the RNN model prediction accuracy at $t = t_k$:

$$E_{rnn}(t_k) = \sum_{i=0}^{N_b} \frac{|x_p(t_{k-i}) - x(t_{k-i})|}{|x(t_{k-i})| + \delta} \quad (9)$$

where N_b is the number of sampling periods before t_k that contribute to the quantification of the prediction error. $x_p(t_{k-i})$ and $x(t_{k-i})$, $i = 0, \dots, N_b$ are the predictions of the past states using RNN models, and the past state measurements from the actual nonlinear system of Eq. 1 under the same control actions, respectively. δ is a small positive real number that is introduced in the denominator of Eq. 9 to avoid the division by small numbers when $x(t_{k-i})$ approaches zero. The RNN model of Eq. 8b is

updated if the accumulated error $E_{rnn}(t_k)$ exceeds the threshold E_T :

$$E_{rnn}(t_k) > E_T \quad (10)$$

where E_T is determined via extensive closed-loop simulations. It should be noted that when an online learning of RNN models is activated, all the data points since the last model update will be used as the training and validation data for the new RNN model. As the number of available data points has a great impact on the RNN model accuracy, N_b and E_T need to be carefully chosen to achieve a desired training performance. Specifically, the moving horizon length N_b is first determined via extensive closed-loop simulations to ensure that there are enough data points that can be utilized in the online update of RNN models, and meanwhile, will not cause data-storage burden. Subsequently, the threshold E_T is determined via simulations off-line to trigger an RNN model update when the state error has accumulated to an undesired level while accounting for common measurement noise, which is sufficiently small compared to time-varying disturbances from model uncertainty, and should not trigger an update of RNN models in most times. Additionally, when the state approaches the unsafe region, the threshold E_T should be adjusted to update online learning more frequently such that the new RNN models are able to capture the most recent dynamics subject to disturbances in a timely manner, and therefore, provide a sufficiently accurate prediction for the CLBF-MPC optimization problem of Eq. 8 to avoid the unsafe region. Lastly, after the RNN model is updated at a certain sampling step $t = t_k$, all the errors before $t = t_k$ are reset to zero.

3.3 Implementation Strategy for On-line RNN Learning Within CLBF-MPC

Based on the error-triggered control scheme proposed in the previous section, the implementation strategy of the on-line RNN learning is integrated with the machine-learning-based CLBF-MPC of Eq. 8 as follows:

Step 1 : An initial RNN model that is utilized in the CLBF-MPC of Eq. 8 is derived from extensive open-loop simulations for the nominal system of Eq. 1 (i.e., $w(t) \equiv 0$) following the construction method in Wu et al. [2019c].

Step 2 : Starting from an initial condition $x_0 \in \mathcal{U}_\rho$, the nonlinear system of Eq. 1 is operated under CLBF-MPC in a sample-and-hold fashion with states being continuously monitored and collected. The online update of RNN models is triggered the moment that the moving horizon error detector of Eq. 9 exceeds its threshold E_T . At the next sampling time, the new RNN model will replace the old model in the CLBF-MPC of Eq. 8 to solve for the optimal control actions $u^*(t)$ for the next sampling period.

Step 3 : When the closed-loop state enters a small neighborhood $\mathcal{U}_{\rho_{min}}$ around the origin, which is considered to be practically stable for the nominal system of Eq. 1, the error-triggering mechanism is taken off-line until the state leaves $\mathcal{U}_{\rho_{min}}$ again due to time-varying disturbances.

Remark 3. It is noted that the online learning of RNN models is performed using the most recent process data only by loading the old RNN models with the previous RNN structure and weight matrices as initialization.

Therefore, the new RNN models that are trained using new data points inherit some important features of the nominal process from the old RNN models and also capture the recent dynamics subject to time-varying disturbances from new data points. Additionally, instead of training a new RNN model from scratch, the training process based on the most recent data and the previous RNN model is more computationally tractable, and thus, can be readily incorporated in the real-time implementation of CLBF-MPC.

4. APPLICATION TO A CHEMICAL PROCESS EXAMPLE

A chemical process example is provided to illustrate the application of machine-learning-based CLBF-MPC to stabilize the closed-loop state at the steady-state and maintain the state in the safe stability region. Specifically, a well-mixed, non-isothermal continuous stirred tank reactor (CSTR) where an irreversible second-order exothermic reaction takes place is considered. The reaction transforms a reactant A to a product B ($A \rightarrow B$). The inlet concentration of A , the inlet temperature and feed volumetric flow rate of the reactor are C_{A0} , T_0 and F , respectively. The CSTR is equipped with a heating jacket that supplies/removes heat at a rate Q . The CSTR dynamic model is described by the following material and energy balance equations:

$$\frac{dC_A}{dt} = \frac{F}{V}(C_{A0} - C_A) - k_0 e^{\frac{-E}{RT}} C_A^2 \quad (11a)$$

$$\frac{dT}{dt} = \frac{F}{V}(T_0 - T) + \frac{-\Delta H}{\rho_L C_p} k_0 e^{\frac{-E}{RT}} C_A^2 + \frac{Q}{\rho_L C_p V} \quad (11b)$$

where C_A is the concentration of reactant A in the reactor, V is the volume of the reacting liquid in the reactor, T is the temperature of the reactor and Q denotes the heat input rate. The concentration of reactant A in the feed is C_{A0} . The feed temperature and volumetric flow rate are T_0 and F , respectively. The liquid has a constant density of ρ_L and a heat capacity of C_p . ΔH , k_0 , E , and R represent the enthalpy of reaction, pre-exponential constant, activation energy, and ideal gas constant, respectively. Process parameter values are in Wu et al. [2019c].

The CSTR is initially operated at the steady-state $x_s = (C_{As}, T_s) = (1.22 \text{ kmol}/\text{m}^3, 438 \text{ K})$, and $u_s = (C_{A0s}, Q_s) = (4 \text{ kmol}/\text{m}^3, 0 \text{ kJ}/\text{hr})$. The manipulated inputs are the inlet concentration of species A and the heat input rate, which are represented by the deviation variables $\Delta C_{A0} = C_{A0} - C_{A0s}$, $\Delta Q = Q - Q_s$, respectively. The manipulated inputs are bounded as follows: $|\Delta C_{A0}| \leq 3.5 \text{ kmol}/\text{m}^3$ and $|\Delta Q| \leq 5 \times 10^5 \text{ kJ}/\text{hr}$. Therefore, the states and the inputs of the closed-loop system are $x^T = [C_A - C_{As} \ T - T_s]$ and $u^T = [\Delta C_{A0} \ \Delta Q]$, respectively, such that the equilibrium point of the system is at the origin of the state-space (i.e., $(x_s^*, u_s^*) = (0, 0)$). In this work, we consider the model variations due to the following disturbances: (1) the feed flow rate F is changing from $5 \text{ m}^3/\text{h}$ to $7 \text{ m}^3/\text{h}$ at $t = 0 \text{ hr}$, and (2) the actual value of the pre-exponential constant k_0 used in the process model is reduced by half to represent a change in the reaction rate at $t = 0 \text{ hr}$.

The control objective is to operate the CSTR process of Eq. 11 at its steady-state while maintaining the closed-loop

state trajectories in the safe stability region \mathcal{U}_ρ using an RNN-based CLBF-MPC scheme. Specifically, we consider an unsafe region \mathcal{D} embedded within the stability region (i.e., a level set of Lyapunov function V) that is defined as an open set, for example, an ellipse described by $\mathcal{D} := \{x \in \mathbf{R}^2 \mid F(x) = (x_1 + 0.92)^2 + \frac{(x_2 - 42)^2}{500} < 0.06\}$. Following the construction method in Wu et al. [2019a], \mathcal{H} is defined as $\mathcal{H} := \{x \in \mathbf{R}^2 \mid F(x) \leq 0.07\}$, and the Control Barrier Function $B(x)$ is designed as follows:

$$B(x) = \begin{cases} e^{\frac{F(x)}{0.07}} - e^{-6}, & \text{if } x \in \mathcal{H} \\ -e^{-6}, & \text{if } x \notin \mathcal{H} \end{cases} \quad (12)$$

Additionally, a Control Lyapunov Function using the standard quadratic form $V(x) = x^T P x$ is constructed with the following positive definite P matrix:

$$P = \begin{bmatrix} 1060 & 22 \\ 22 & 0.52 \end{bmatrix} \quad (13)$$

Therefore, $W_c(x) = V(x) + \mu B(x) + \nu$ is designed with the following parameters $\rho_c = 0$, $c_1 = 0.1$, $c_2 = 1061$, $c_3 = \max_{x \in \partial \mathcal{H}} |x|^2 = 2295$, $c_4 = \min_{x \in \partial \mathcal{D}} |x|^2 = 1370$. $\nu = \rho_c - c_1 c_4 = -160$, and $\mu = 1 \times 10^9$ to meet the conditions of CLBFs in Eq. 5.

The explicit Euler method with an integration time step of $h_c = 2 \times 10^{-5} \text{ hr}$ is applied to numerically simulate the dynamic model of Eq. 11. The nonlinear optimization problem of the RNN-based CLBF-MPC of Eq. 8 is solved using the IPOPT software package Wächter and Biegler [2006] and its Python version, named, PyIpop, with the sampling period $\Delta = 2 \times 10^{-3} \text{ hr}$.

The closed-loop simulation of the CSTR of Eq. 11 is carried out under the CLBF-MPC with and without online learning of RNN models, respectively, and the results are shown in Figs. 1-3. Specifically, in Fig. 1, it is demonstrated that in the presence of disturbances, the closed-loop state trajectory under the CLBF-MPC using online update of RNN models is able to avoid the unsafe region and converge to a small neighborhood around the origin, while the one under the CLBF-MPC without online RNN update crosses the red unsafe region \mathcal{D} due to a considerable model mismatch between the initial RNN model for the nominal process of Eq. 11 and the actual process subject to disturbances. Fig. 2 shows the input profiles under the CLBF-MPC with and without online RNN update, from which recursive feasibility and satisfaction of input constraints are demonstrated for both optimization. Additionally, it is also observed in Fig. 2 that since RNN models are updated in a timely manner under the CLBF-MPC with online learning, the oscillation of u_1 becomes less near the end of operation period compared to the one without online update.

The value of error is shown in Fig. 3 for CLBF-MPCs with and without online RNN update. It is demonstrated that without online learning, the error exceeds the threshold quickly and increases to an undesired level during the operation, which implies the failure of the initial RNN model in capturing the actual CSTR dynamics in the presence of disturbances. However, under the CLBF-MPC with online RNN learning, it is demonstrated that the RNN model update is triggered six times during the entire operation period (i.e., $t=0.06 \text{ hr}$) to maintain the error

below its threshold for most of the time. Therefore, with online learning, the RNN models used in CLBF-MPC always capture the latest process dynamics subject to disturbances, and lead to a desired closed-loop performance for the CSTR of Eq. 11 with simultaneous closed-loop stability and operational safety.

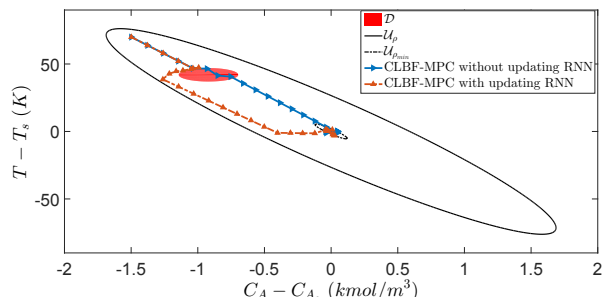


Fig. 1. The state-space profiles for the closed-loop CSTR subject to time-varying disturbances under the CLBF-MPC of Eq. 8 with (red trajectory) and without online RNN update (blue trajectory), respectively, for an initial condition $(-1.5, 70)$.

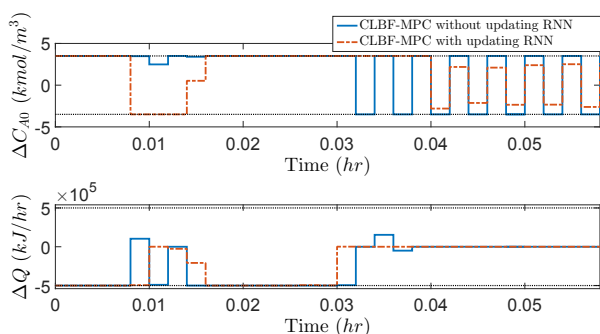


Fig. 2. Manipulated input profiles ($u_1 = \Delta C_{A0}$, $u_2 = \Delta Q$) for the closed-loop CSTR subject to time-varying disturbances under the CLBF-MPC of Eq. 8 with (red trajectory) and without online RNN update (blue trajectory), respectively, for an initial condition $(-1.5, 70)$.

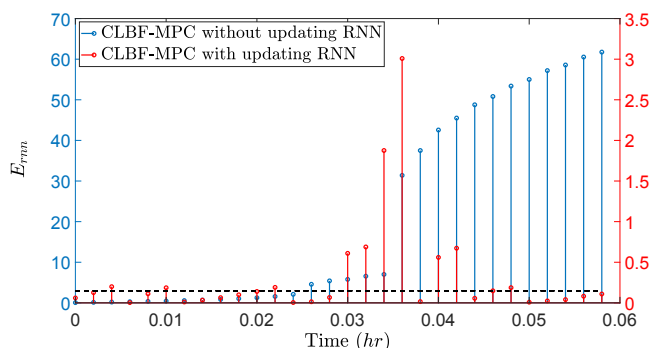


Fig. 3. Value of $E_{rnn}(t)$ at each sampling time for the closed-loop CSTR subject to time-varying disturbances under the CLBF-MPC of Eq. 8 with (red, right y-axis) and without online RNN update (blue, left y-axis), respectively, where the threshold E_T is set to 0.15.

5. CONCLUSION

In this work, we proposed a real-time machine learning-based CLBF-MPC scheme using error-triggered online learning of RNN models to optimize process operational safety and closed-loop stability for nonlinear systems subject to time-varying disturbances. The application to a chemical reactor example demonstrated that the closed-loop state was able to avoid the unsafe region and converged to a small neighborhood around the origin under the CLBF-MPC with online update of RNN models.

REFERENCES

- Ames, A.D., Xu, X., Grizzle, J.W., and Tabuada, P. (2016). Control barrier function based quadratic programs with application to automotive safety systems. *arXiv preprint arXiv:1609.06408*.
- Jankovic, M. (2017). Combining control Lyapunov and barrier functions for constrained stabilization of nonlinear systems. In *Proceedings of the American Control Conference*, 1916–1922. Seattle, Washington.
- Kosmatopoulos, E.B., Polycarpou, M.M., Christodoulou, M.A., and Ioannou, P.A. (1995). High-order neural network structures for identification of dynamical systems. *IEEE Transactions on Neural Networks*, 6, 422–431.
- Lin, Y. and Sontag, E.D. (1991). A universal formula for stabilization with bounded controls. *Systems & Control Letters*, 16, 393–397.
- Romdlony, M.Z. and Jayawardhana, B. (2016). Stabilization with guaranteed safety using control Lyapunov-barrier function. *Automatica*, 66, 39–47.
- Sontag, E.D. (1989). A ‘universal’ construction of Artstein’s theorem on nonlinear stabilization. *Systems & Control Letters*, 13, 117–123.
- Trischler, A.P. and D’Eleuterio, G.M. (2016). Synthesis of recurrent neural networks for dynamical system simulation. *Neural Networks*, 80, 67–78.
- Wächter, A. and Biegler, L.T. (2006). On the implementation of an interior-point filter line-search algorithm for large-scale nonlinear programming. *Mathematical Programming*, 106, 25–57.
- Wu, Z., Albalawi, F., Zhang, Z., Zhang, J. and Durand, H., and Christofides, P.D. (2019a). Control Lyapunov-Barrier function-based model predictive control of nonlinear systems. *Automatica*, 109, 108508.
- Wu, Z. and Christofides, P.D. (2020). Control Lyapunov-barrier function-based predictive control of nonlinear processes using machine learning modeling. *Computers & Chemical Engineering*, 134, 106706.
- Wu, Z., Rincon, D., and Christofides, P.D. (2019b). Real-time adaptive machine-learning-based predictive control of nonlinear processes. *Industrial & Engineering Chemistry Research*, 59, 2275–2290.
- Wu, Z., Tran, A., Rincon, D., and Christofides, P.D. (2019c). Machine learning-based predictive control of nonlinear processes. part I: Theory. *AIChE Journal*, 65, e16729.
- You, Y. and Nikolaou, M. (1993). Dynamic process modeling with recurrent neural networks. *AIChE Journal*, 39, 1654–1667.